ELSEVIER

Gene Expression Patterns 5 (2005) 609–617

GEP

www.elsevier.com/locate/modgep

Adamts9 is widely expressed during mouse embryo development☆

Katherine A. Jungers, Carine Le Goff, Robert P.T. Somerville, Suneel S. Apte*

Department of Biomedical Engineering and Orthopaedic Research Center, Lerner Research Institute, Cleveland Clinic Foundation (ND20), 9500 Euclid Avenue, Cleveland, OH 44195, USA

Received 8 October 2004; received in revised form 4 March 2005; accepted 11 March 2005
Available online 20 April 2005

Abstract

ADAMTS metalloproteases constitute a family of 19 secreted protein or proteoglycan processing enzymes. ADAMTS9 and its closest mammalian relative, ADAMTS20, are related to gon-1, a metalloprotease required for gonadal morphogenesis in *Caenorhabditis elegans*. Although expressed at generally low levels in embryonic subectodermal mesenchyme, ADAMTS20 is required for melanoblast colonization of skin. Mutations in *Adamts20* cause *Belted*, one of several white spotting alleles in the mouse. In contrast to *Adamts20*, we previously showed by Northern blotting that *Adamts9* was expressed highly throughout mouse development. Using RNA in situ hybridization, we determined the spatial and temporal regulation of *Adamts9* during mouse embryogenesis. At 7.5 dpc *Adamts9* is expressed in the allantois, trophoblast, parietal endoderm and decidual tissue. At 9.5 dpc it is expressed in head mesoderm and in the developing heart. From 11.5 to 12.5 dpc, *Adamts9* is strongly expressed in posterior mesoderm, in the craniofacial region, ventral body wall and diaphragm. After 14.5 dpc, *Adamts9* was highly expressed in the mesenchyme of developing lung, kidney, and mesentery. It is expressed during skeletogenesis, being present from 13.5 dpc in perichondrium, in the proliferation zone of growth plates after 15.5 dpc and it is highly expressed in newly formed bone. It is expressed in vascular endothelium and during formation of the pituitary and cochlea, but expression in the central nervous system is limited to the floor plate of the diencephalon, to the ventricular zone of the cerebral cortex and to the choroid plexus.

Keywords: ADAMTS; Metalloprotease; ADAMTS9; ADAMTS20; gon-1; Aggrecan; Versican; Belted; In situ hybridization; Mouse; Embryogenesis; Mesoderm; Rathke's pouch; Trophoblast; Endochondral ossification

1. Results and discussion

ADAMTS (a disintegrin-like and metalloprotease domain with thrombospondin type 1 repeats) is a family of 19 secreted mammalian metalloproteases (Apte, 2004). Natural or transgenic mutations in ADAMTS1, 2, 10, and 20 have revealed important developmental roles for these proteases (Colige et al., 1999; Dagoneau et al., 2004; Rao et al., 2003; Shindo et al., 2000). However, the functions of the majority of ADAMTS proteases are unclear. Only one ADAMTS protease in *Caenorhabditis elegans* and *Drosophila melanogaster* has a clearly identifiable ortholog in humans and mice. This enzyme, named gon-1 in *C. elegans*, has considerable sequence similarity with human and mouse ADAMTS9 and ADAMTS20 (Blelloch and Kimble, 1999; Llamazares et al., 2003; Somerville et al., 2003). The hallmark of these three enzymes is the presence of a distinctive C-terminal module. Both the overall sequence and the cysteine signature of this so-called gon-1 module are highly conserved in ADAMTS9 and ADAMTS20, which comprise a distinct ADAMTS subfamily. Such stringent evolutionary conservation suggests important biological roles for ADAMTS9 and ADAMTS20 in mammals.

Recently, it was shown that naturally occurring mutations in *Adamts20* resulted in a mouse phenotype named *Belted*, owing to an essential role for ADAMTS20 in neural-crest-derived melanoblast migration through dermal mesenchyme or survival and proliferation within

Abbreviations: ADAMTS, a disintegrin-like and metalloprotease domain with thrombospondin type 1 motifs; PCR, polymerase chain reaction; bp, base pairs; dpc, days post-coitum; TSR, thrombospondin type 1 repeat.

☆ Gene nomenclature has been assigned in agreement with the Human and Mouse Gene Nomenclature Committees. As an example, *ADAMTS9* and *Adamts9* are human and mouse orthologs. The protein products of both genes are designated as ADAMTS9. Similar nomenclature is used for other ADAMTS genes and their products.

* Corresponding author. Tel.: +1 216 445 3278; fax: +1 216 444 9198.
E-mail address: aptes@ccf.org (S.S. Apte).

1567-133X/$ - see front matter © 2005 Elsevier B.V. All rights reserved.
doi:10.1016/j.modgep.2005.03.004

the ectoderm (Rao et al., 2003). *Adamts20* was specifically expressed in the subectodermal mesenchyme during development, yet its overall expression as determined by Northern blotting was quite meagre (Rao et al., 2003; Somerville et al., 2003; Llamazares et al., 2003). On the other hand, *Adamts9* is highly expressed throughout mouse embryo development and continues to be expressed in a variety of adult tissues as determined by Northern blot and RT-PCR analysis (Clark et al., 2000; Somerville et al., 2003). Here, we determined the precise spatial and temporal expression of *Adamts9* using radioactive RNA in situ hybridization. Specific hybridization to the antisense riboprobe suggested potential roles in several important biological processes.

Sense cRNA probe did not give autoradiographic signal above background levels (Fig. 9H). In addition, the hybridization signal was different from that previously reported for ADAMTS20 (Rao et al., 2003), a homolog with highest sequence similarity to ADAMTS9. Other ADAMTS proteases whose developmental expression we have determined have very different expression profiles in situ, suggesting that there was no cross-hybridization to other ADAMTS proteases.

1.1. Expression within the peri-implantation period and early embryogenesis (7.5–9.5 dpc)

At 7.5 dpc, *Adamts9* was expressed both within fetal and maternal tissues (Fig. 1A). There was strong expression in trophoblast giant cells and the parietal endoderm (Fig. 1A,B). In the embryonic part of the conceptus, there was strongly localized expression to the region of the allantois (Fig. 1B). On the maternal side, expression was present in the decidual reaction, as well as within the myometrium and in the uterine artery (Fig. 1A,C,D). Within the decidual reaction, *Adamts9* was expressed in the capillaries, including the endothelium (Fig. 1C). The expression within the maternal tissues and extra-embryonic part of the conceptus was more prominent than expression within the embryo proper.

At 9.5 dpc, expression in the trophoblast, parietal endoderm, uterine myometrium and decidual reaction continued (Fig. 2A–C). In sagittal sections of the 9.5 dpc embryo, prominent expression was seen in the heart tube and mesoderm of the first branchial arch and head (Fig. 2D,E).

1.2. Expression from 11.5 to 12.5 dpc

Sagittal sections at these stages showed that *Adamts9* was strongly expressed in mesoderm (Fig. 3A–C); expression in the ventral body wall was particularly strong and was localized to the subectodermal mesenchyme. At 11.5 dpc, strong expression was seen along the presumed migratory pathway of cardiac neural crest cells and limb and hypoglossal muscle precursors as well as in ventral tail mesoderm (Fig. 3A,B). A transverse section at the level of the developing heart confirmed strong expression along the known migration pathways of cardiac and vascular neural crest cells (NCC) and limb muscle precursors of

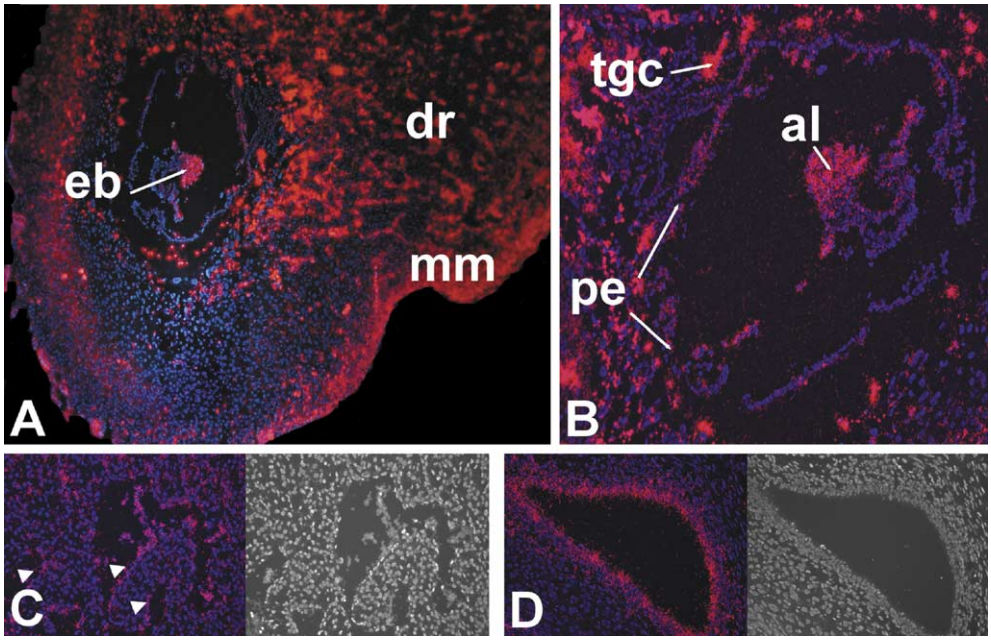

Fig. 1. Expression of *Adamts9* in maternal and fetal tissues at 7.5 dpc. (A) Low magnification view of decidua at 7.5 dpc showing intense signal in the myometrium (mm), in the decidual reaction (dr) and the embryo (eb). (B) The embryonic expression is in the allantois (al), parietal endoderm (pe) and trophoblast giant cells (tgc). (C) Localization of *Adamts9* in the uterine deciduum at 7.5 dpc. Comparison with Hoechst 33258 labeled image of this section on the right suggests signal localization to vascular endothelium (arrowheads). (D) Uterine artery from 7.5 dpc gravid uterus showing strong signal in the arterial wall and endothelium (fluorescent image is shown at right for comparison).

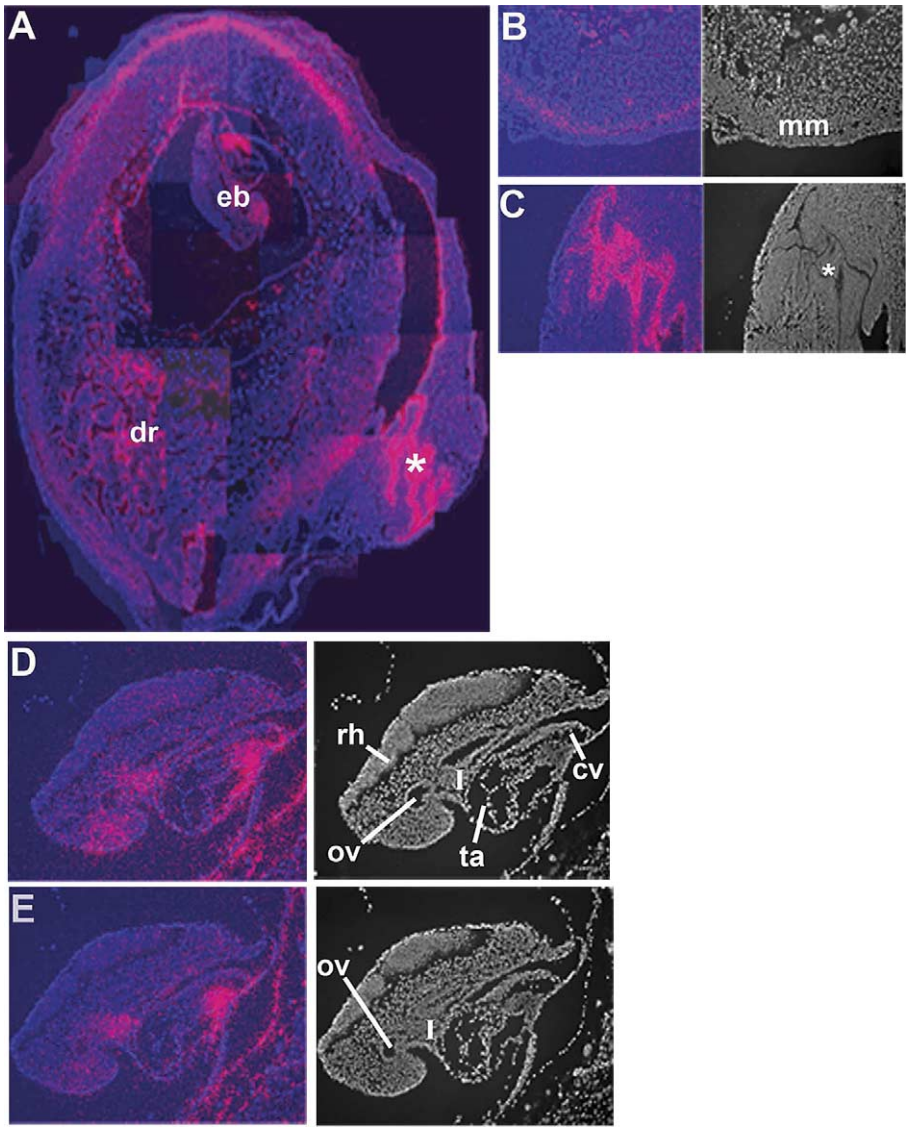

Fig. 2. Expression of *Adamts9* in maternal and fetal tissues at 9.5 dpc (A–E). (A) View of the entire uterus at 9.5 dpc showing signal in the decidual reaction (dr), residual uterine lumen (asterisk) and the embryo (eb). (B) Localization of *Adamts9* in the myometrium (mm). (C) Intense expression is seen in the epithelium of the residual uterine cavity (asterisk). (D and E) Localization of *Adamts9* in the developing embryo from two para-sagittal sections showing strong staining in the first branchial arch (I), in head mesoderm near the optic vesicle (ov) and common ventricle (cv). Low expression is present in the wall of the truncus arteriosus (ta). Note absence in rhombomeres (rh). Corresponding fluorescent images are shown at right for comparison.

the forelimb (Fig. 3A). Since ADAMTS20 participates in migration of a subset of NC-derived cells, i.e. melanoblasts, these observations are quite intriguing. Particularly, strong expression was noted around the cardinal veins and the dorsal aorta (Fig. 3A) as well as around the umbilical vessels (Fig. 3B). Radioactive signal was detected within the myocardium and the walls of cardiac outflow tract (Fig. 3A,B inset). Low levels of expression were seen in craniofacial mesenchyme (discussed below in the context of pituitary development) (Fig. 3B) at 11.5 dpc. At 12.5 dpc the cervical mesoderm expression had increased in relative intensity and advanced further anteriorly and into craniofacial mesenchyme (Fig. 3C).

1.3. Expression from 13.5 to 15. 5 dpc

These three developmental stages showed broadly similar expression profiles and can be summed up by illustrating expression at 14.5 dpc (Fig. 4A). Expression in diaphragm and ventral body wall noted in the earlier stages continued, but stronger expression became apparent in the mesenchyme of the genital tubercle, lungs, heart, kidney, pancreas, gonad, developing urinary bladder, stomach, intestines and adrenal capsule (Fig. 4A–C). The tunica media of intestines, craniofacial mesenchyme around the developing pituitary, cochlea, pharynx and nasal sinuses and the ossification centers in the mandible

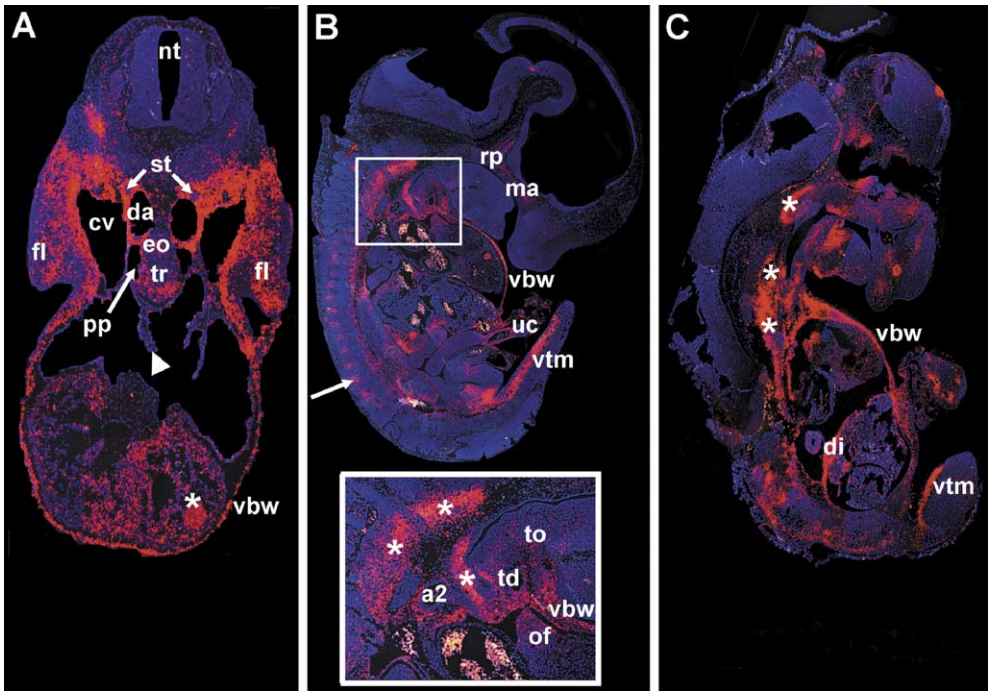

Fig. 3. (A–C) Expression of *Adamts9* in the 11.5–12.5 dpc mouse embryo. (A) Transverse section through the thorax of an 11.5 dpc embryo. (B) Sagittal section through an 11.5 dpc embryo. The boxed area is shown at higher magnification in the inset. (C) Sagittal section through a 12.5 dpc embryo. Figure annotation is as follows: da, dorsal aorta; di, diaphragm; eo, esophagus; fl, forelimb; ma, maxilla; nt, neural tube; pp, pleuroperitoneal canal; rp, Rathke's pouch; st, sympathetic trunk; tr, trachea; uc, umbilical cord; vbw, ventral body wall; vtm, ventral tail mesoderm. The arrowhead in (A) indicates the edge of the septum primum and the asterisk shows a signal artifact. The arrow in (B) indicates signal in early pre-cartilage condensations. The boxed area in (B) is enlarged in the area of branchial arches I and II to better illustrate the signal localization to these areas. In the inset, a2 indicates the artery of the second branchial arch; td, the thyroglossal duct; of, the endocardial cushion of the pulmonary outflow tract; to, tongue. The asterisks indicate strong signal in migrating mesodermal cells, possibly muscle precursors.

expressed *Adamts9* (Fig. 4A). Expression was also noted from 13.5 to 15.5 dpc in the perichondrium of rib cartilage. Limited expression within the central nervous system was seen in the ventricular zone of the developing cerebral hemispheres and within the mesenchyme core of the choroid plexus (Figs. 4A, 7A). Within the developing limbs, *Adamts9* was strongly expressed in the mesenchyme around cartilage but at low levels in the cartilage itself (Fig. 4B,C). The strong signal noted in the tail mesoderm at earlier stages resolved into expression within the tail tendons (Fig. 4A–C).

1.4. Expression at 17.5 dpc

Adamts9 peaked in several locations at this late developmental stage, with the strongest expression in mesenchyme of lung and kidney (Fig. 5). There was significant expression in the mandible and other ossification centers, and the cochlear connective tissue (Fig. 5). There was a relative decrease in expression within the diaphragm and ventral body wall compared to earlier stages.

1.5. Expression during pituitary development

Adamts9 showed a dynamic expression pattern during pituitary development (Fig. 6) where it was expressed both within the epithelium of Rathke's pouch as well as the surrounding mesenchyme. Interestingly, the pharyngeal ectoderm from which Rathke's pouch is derived did not express *Adamts9*, indicative of a change in phenotype of the migrating epithelial derivative.

1.6. Expression within the vasculature

Adamts9 was present in endothelium lining capillaries (Figs. 1A, 6D, 7A) as well as in the wall of arteries (Figs. 1D, 7B,C). Expression in the umbilical arteries, which are of allantoic origin, occurred throughout development, which is interesting in view of the early expression in allantois.

1.7. Expression within glandular and visceral organs

Adamts9 had a striking expression in the mesenchyme of numerous epithelial organs, such as the lung, submandibular salivary gland, kidney and intestines each of which undergoes most of its morphogenesis from 12.5 to 17.5 dpc (Fig. 8A–D). In the abdominal cavity, *Adamts9* was strongly expressed in the developing peritoneum (Figs. 8D, 9A,B), and in the mesenteric supports of the gut (Fig. 9A,B).

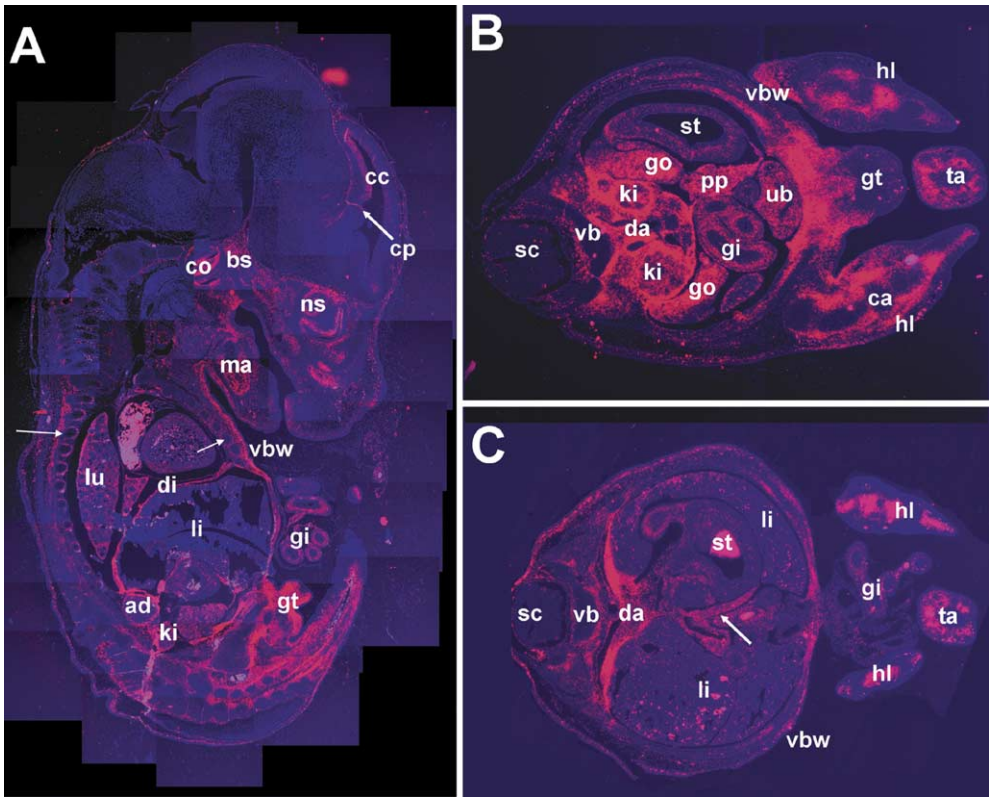

Fig. 4. Expression of *Adamts9* in the 13.5–14.5 dpc mouse embryo. (A) Sagittal section through a 14.5 dpc embryo. The thin arrows indicate signal in rib and sternal perichondrium. Note the strong signal in the mesenchyme in the region of the genital tubercle (gt) and tail mesoderm that is also seen in (B) and (C) and localizes *Adamts9* signal to tail tendons. (B,C) Transverse sections through the abdomen (13.5 and 14.5 dpc, respectively). Sections at different levels through the hindlimbs in (B) and (C) illustrate that *Adamts9* is not expressed in the cartilage models (ca) of the limb bones but primarily in the surrounding connective tissue (perichondrium, muscle and tendon). The arrow in (C) points to the portal vein. Note the strong signal in posterior abdominal mesenchyme around the great vessels in (B) and (C). Figure annotation is as follows: ad, adrenal gland; bs, basi-sphenoid; co, cochlea; ca, cartilage; cc, cerebral cortex; cp, choroids plexus; da, aorta; di, diaphragm; go, gonad; gi, gastrointestinal tract; gt, genital tubercle; hl, hindlimb; ki, kidney; lu, lung; li, liver; ma, mandible; ns, nasal sinuses; pp, pancreas; sc, spinal cord; st, stomach; ub, urinary bladder; ta, tail; vb, vertebral body; vbw, ventral body wall.

1.8. Expression during skeletal development

Skeletal development occurs entirely within the second half of gestation. In early stages (11.5–14.5 dpc), *Adamts9* was associated first with the initial condensations of mesenchyme that forms the cartilage centers and subsequently with the perichondrium around formed cartilage (Fig. 10A–D). Perichondrium expression is significant since ADAMTS9 is capable of degrading versican, an important component of this tissue (Shinomura et al., 1993). After 15.5 dpc, *Adamts9* was detected in the proliferative zones of growth cartilage, both in the vertebral end-plate (Fig. 10E) and long bones, as shown in the proximal femur (Fig. 10F). Once endochondral ossification occurred, extremely strong expression was seen in newly formed bone, as shown in the mandible at 15.5 dpc and ribs at 17.5 dpc (Figs. 4, 5 and 10G,H). The precise cell types expressing *Adamts9* in bone, however, were not identified, although their location on the surface of bone suggests they may be osteoblasts. *Adamts9* was expressed during tooth development, most strongly in the tooth socket, and to a lesser extent in the developing tooth itself (Fig. 10I).

1.9. Expression in nervous system and sensory organs

Compared to its strong expression in connective tissue and visceral organs, *Adamts9* was relatively sparsely expressed in the CNS at all developmental stages examined, except for transient expression in the floorplate of the diencephalon (12.5 dpc, Fig. 3C), cerebral cortex (14.5 dpc, Fig. 4A), dorsal root ganglia (15.5 dpc onwards, Fig. 10C) and choroid plexus (Fig. 6A). It was expressed throughout cochlear development within connective tissue surrounding the neuroepithelium. In relation to the olfactory system, it was strongly expressed in mesenchyme around the nasal epithelium. We have not examined expression in the eye.

1.10. Comparison with the expression profile of other ADAMTS proteases

Since ADAMTS9 is activated by pro-protein convertases in the secretory pathway or at the cell surface (Somerville et al., 2003) and because there are few known endogenous ADAMTS inhibitors, it is likely that transcriptional regulation is an important control mechanism.

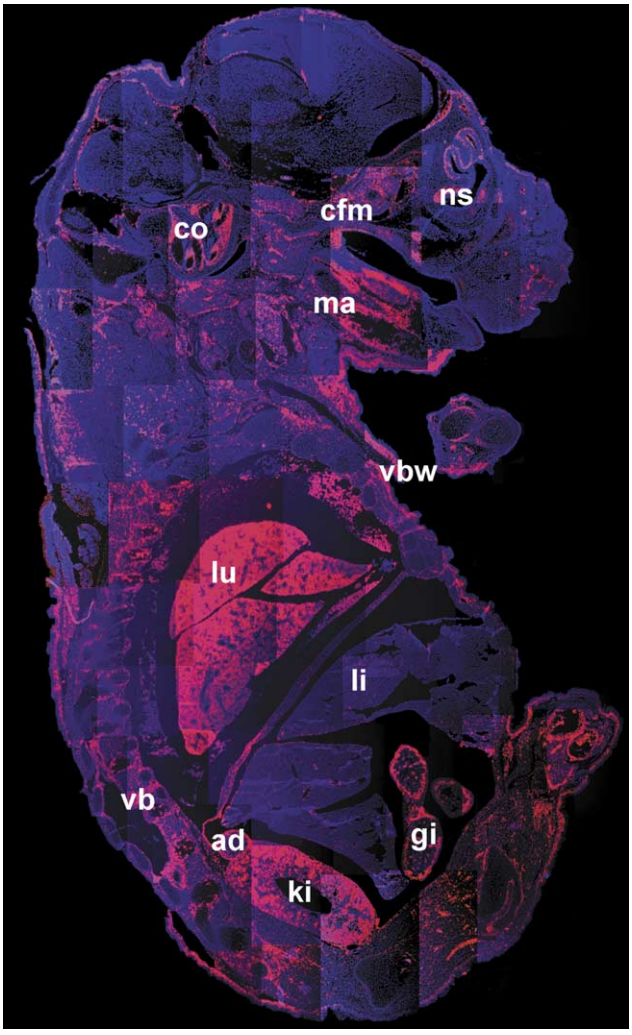

Fig. 5. Expression of *Adamts9* in the 17.5 dpc mouse embryo. A sagittal section is illustrated. The grid-like appearance of the image is a result of assembly from a large number of smaller individual images. Figure annotation is as follows: ad, adrenal gland; co, cochlea; cfm, craniofacial mesenchyme; gi; gastrointestinal tract; ki, kidney; li, liver; lu, lung; ma, mandible, ns, nasal sinuses; vb, vertebral body; vbw, ventral body wall.

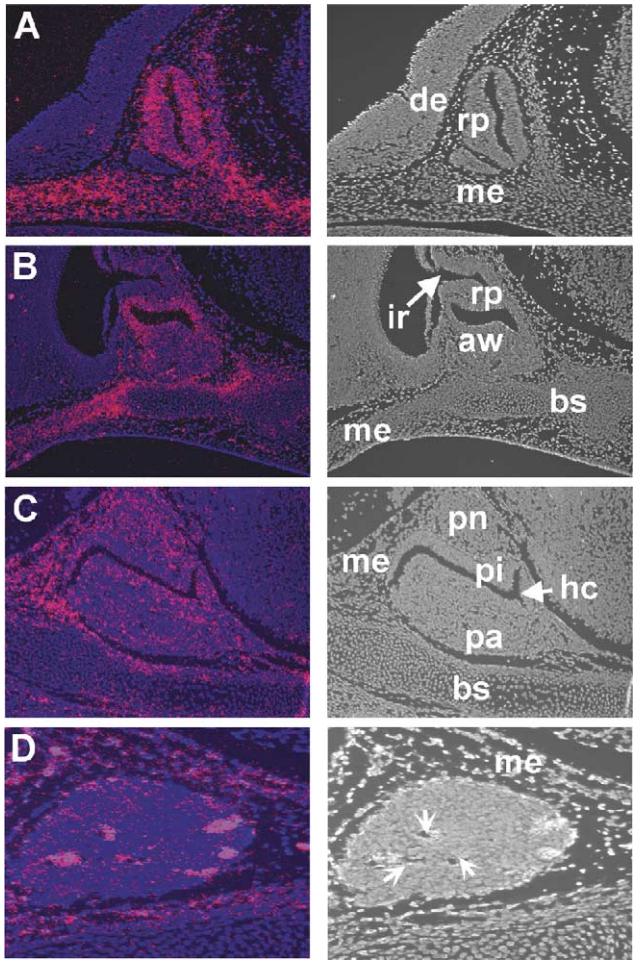

Fig. 6. Expression of *Adamts9* during pituitary development. The right panel shows the nuclear fluorescence alone to provide a structural correlate. (A) Expression is seen at 11.5 days in the Rathke's pouch epithelium (rp), and in the mesenchyme (me) of the pharynx, but not in the pharyngeal ectoderm or the diencephalon (de). (B) At 13.5 dpc, *Adamts9* is expressed in the Rathke's pouch remnant epithelium (rp) and in the anterior wall (aw) of the pars intermedia. Expression continues in the mesenchyme above the pharynx (me) but is not seen in the basi-sphenoid cartilage (bs); ir denotes the infundibular recess. (C) Expression at 15.5 dpc is seen in the pars nervosa (pn), the pars intermedia (pi) and the pars anterior (pa) as well as in the surrounding mesenchyme (me). The hypophyseal cleft (hc), the remnant of the lumen of Rathke's pouch, is indicated. (D) By 17.5 dpc, when pituitary development is complete, expression is restricted to its vasculature (arrows), although it continues in the surrounding mesenchyme (me).

In addition, since members of ADAMTS subfamilies appear to have similar biochemical properties, their transcriptional regulation relative to each other becomes critical in determining functional redundancy and specificity (Apte, 2004) site.

A comprehensive study of *Adamts1* expression showed it to be expressed predominantly in epithelium of the developing lung, pancreas, kidney, skin appendages and choroid plexus as well as within a subset of developing neurons, and the walls of large arteries. Thus, *Adamts1* expression in most locations other than the arterial wall and perichondrium complements, but does not overlap with that of *Adamts9*. Interestingly, both ADAMTS1 and ADAMTS9 process versican, which is a major component of the arterial wall and perichondrium, and aggrecan, which is a major cartilage proteoglycan. *Adamts9* expression in the proliferating zone of growth plate could indicate a role in aggrecan turnover; interestingly, of the ADAMTS proteases that can process aggrecan, *Adamts9* is the first to be identified in developing cartilage. Two other versican processing enzymes, ADAMTS4 and ADAMTS5, are somewhat closely related to ADAMTS9, but not to the same degree as ADAMTS20. *Adamts4* is not expressed at detectable levels during mouse embryogenesis (K.A. Jungers and S.S. Apte, unpublished observation). We recently completed a comprehensive developmental expression

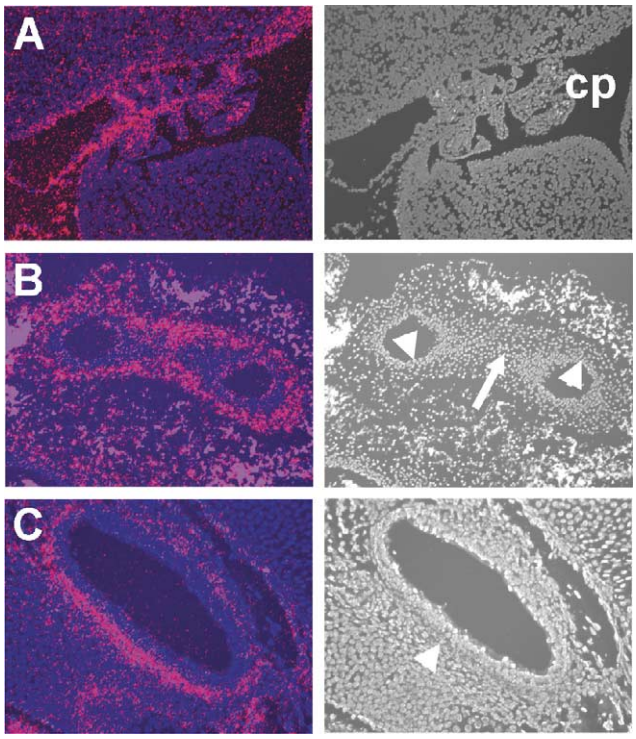

Fig. 7. Expression of *Adamts9* in blood vessels. The right panel shows the nuclear fluorescence alone to provide a structural correlate. (A) Choroid plexus (cp) from 15.5 dpc brain showing signal localized to the vascular core, but not to the epithelium. (B) Umbilical vessels from 15.5 dpc embryo showing expression in the wall (arrow) as well as the vascular endothelium (arrowheads). (C) Expression within the carotid artery showing localization to the arterial wall.

analysis of *Adamts5* mRNA (C. Legoff, S. Apte, manuscript in preparation), which has a different distribution from that of *Adamts9*. Our unpublished studies of developmental expression of the three procollagen amino-propeptidase genes, *Adamts2*, *Adamts3* and *Adamts14*, uncovered a high degree of co-expression with their fibrillar collagen substrates, again quite different from *Adamts9*. *Adamts9* is not expressed at significant levels in the liver, unlike *Adamts13*, the von Willebrand factor protease (Zheng et al., 2001). Recently, we demonstrated widespread mesenchymal expression of *Adamts10*, the enzyme mutated in recessive Weill-Marchesani syndrome (Somerville et al., 2004). The present studies demonstrate exceptionally strong and widespread mesenchymal expression of *Adamts9*, overlapping in several places with *Adamts10* (Somerville et al., 2004). However, such overlap does not imply functional redundancy since ADAMTS9 and ADAMTS10 differ in their domain structure and active site sequence;

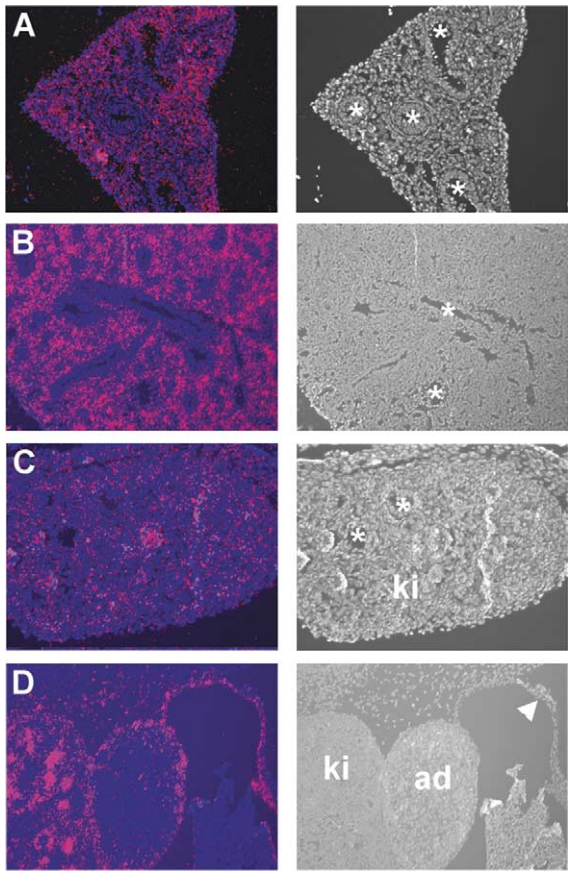

Fig. 8. Expression of *Adamts9* in lung and kidney. (A and B) Expression is shown in lung development at 13.5 dpc (A) and 17.5 dpc (B). Note that expression is absent in the epithelium lining bronchial tubes (asterisks) but is present in the surrounding mesenchyme. (C and D) Expression is shown within the developing kidney at 15.5 dpc (C) and 17.5 dpc (D). Note exclusion of signal from tubular epithelium (asterisk). In the adrenal gland (ad), *Adamts9* mRNA is mostly found in the capsule and in the peritoneal reflection onto the posterior abdominal wall (arrowhead).

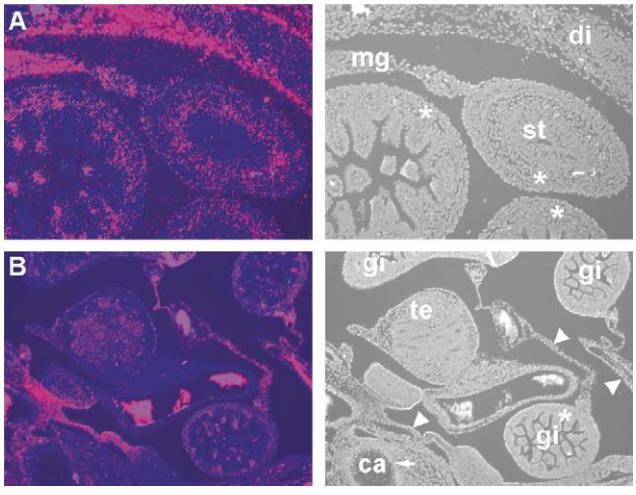

Fig. 9. *Adamts9* expression in the peritoneum and mesentery of abdominal viscera. The right panel shows the nuclear fluorescence alone to provide a structural correlate. (A) In the 15.5 dpc embryo, strong signal is seen in the mesogastrium (mg, the supporting mesentery of the stomach), the diaphragm (di) as well within the muscular wall (tunica media) of the stomach and adjacent intestines (asterisks). (B) At 17.5 dpc, strong expression continues in mesentery (arrowheads), the muscular wall of the intestines (asterisk), and testis (te), and is particularly strong within the posterior peritoneum as it is reflected onto the mesonephros on the bottom left. Note that the cartilage (ca) is negative, but *Adamts9* is located in its perichondrium (arrow).

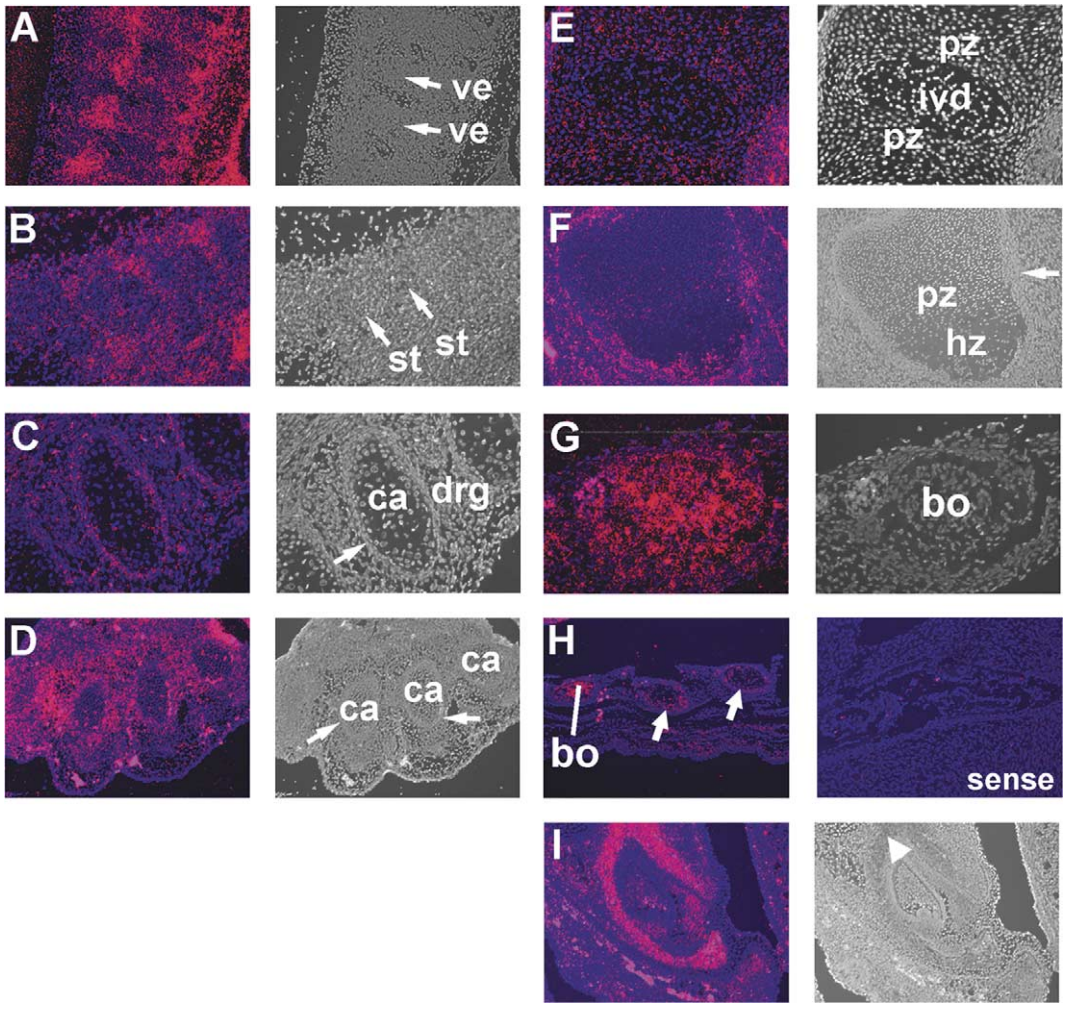

Fig. 10. *Adamts9* expression in the developing skeleton. (A) *Adamts9* is expressed in the precartilaginous mesenchymal condensations that will form the ribs and vertebrae (ve) at 11.5 dpc. (B) Once the first chondrocytes are formed as shown here in the sternum (st) at 12.5 dpc, *Adamts9* is expressed in the perichondrium (st). (C and D) Expression in the perichondrium is shown by arrows in the ribs (C) and metacarpals of the forepaw (cross-section in D) at 15.5 dpc. ca, cartilage and drg, dorsal root ganglion. (E) At 17.5 dpc, there is specific and significant expression in the proliferating chondrocytes (pz) in the vertebral end-plates (E) but no expression is found in the intervertebral disc (ivd). (F) In the 17.5 dpc proximal femur expression is present in the perichondrium (arrow) and proliferative zone (pz) but not in the hypertrophic zone (hz). (G) Once ossification commences, *Adamts9* is expressed very strongly in bone (bo), as shown in the 17.5 dpc mandible. (H) In the 17.5 day sternum, strong expression in bone (bo) contrasts with absent expression in cartilage of adjacent unossified segments (arrows) (H, left panel). The right-hand panel in (H) shows the lack of hybridization to a sense probe. (I) Expression in the uninterrupted lower incisor at 17.5 dpc is highest in the socket (arrowhead), but not as prominent within the tooth bud itself.

we have shown that unlike ADAMTS9, ADAMTS10 processes neither aggrecan nor versican (Somerville et al., 2004). However, functional redundancy could occur in those locations, where *Adamts9* and *Adamts20* expression domains overlap. Thus, expression of *Adamts9* in subectodermal mesenchyme may compensate for *Adamts20* mutations in *Belted* and limit the white spotting to a narrow belt around the torso. Overall, it is interesting that *Adamts9* is strongly expressed along the pathways of migration and colonization of neural crest-derived cells in regions as diverse as the branchial arches, the major arteries and in the mesentery and walls of the intestine. These locations raise the possibility, that like ADAMTS20 and gon-1, but in a much broader developmental context, ADAMTS may also support cell migration during development.

2. Methods

2.1. Embryos and sections

Mouse embryos were collected from crosses of C57/Bl6 mice. The morning of the vaginal plug was designated 0.5 days post-coitum (dpc). Embryos of age 7.5, 9.5, 11.5, 12.5, 13.5, 14.5, 15.5 and 17.5 dpc were used in these studies. Mouse embryos were immediately fixed in 4% paraformaldehyde in phosphate-buffered saline, pH 7.2 and embedded

in paraffin. 5–7 μM sections were used for in situ hybridization.

2.2. Adamts9 riboprobe preparation

A partial *Adamts9* cDNA clone MT3-33 was obtained during efforts to clone full-length mouse ADAMTS9. A 715 bp EcoRI–XbaI cDNA fragment from this clone encoding the cysteine-rich module, spacer and TSRs 2–4 was cloned into pBluescript SK+ (Stratagene). The plasmid was linearized with EcoRI and XbaI for in vitro transcription using T7 and T3 RNA polymerases to provide anti-sense and sense cRNA probes, respectively. The sense probe was used as a control to determine specificity of hybridization of the anti-sense probe. Labeling was done in the presence of {35S}-UTP to provide continuously labeled radioactive cRNA probes.

2.3. Section radioactive in situ hybridization

Hybridization was done essentially as previously described (Somerville et al., 2003). After hybridization, sections were dipped in NTB-2 emulsion (Kodak, Rochestor, NY) for autoradiography. Following the development of photographic emulsion, nuclei were stained with the fluorescent dye Hoechst 33258 (Sigma). Sections were viewed under dark field illumination to identify silver grains and under UV light to image the nuclei. A cooled CCD camera was used to obtain dark-field and fluorescent images of the same field. Signal from dark-field microscopy was given a red pseudocolor and these pseudocolored images were overlaid on the fluorescent images.

Acknowledgements

This work was supported by NIH award AR 49930 (to S. Apte) and assisted in part by NIH award AR 050953 (which established the Cleveland Clinic Foundation Core Center for Musculoskeletal disorders).

References

Apte, S.S., 2004. A disintegrin-like and metalloprotease (reprolysin type) with thrombospondin type 1 motifs: the ADAMTS family. Int. J. Biochem. Cell Biol. 36, 981–985.

Blelloch, R., Kimble, J., 1999. Control of organ shape by a secreted metalloprotease in the nematode *Caenorhabditis elegans*. Nature 399, 586–590.

Clark, M.E., Kelner, G.S., Turbeville, L.A., Boyer, A., Arden, K.C., Maki, R.A., 2000. ADAMTS9, a novel member of the ADAM-TS/metallospondin gene family. Genomics 67, 343–350.

Colige, A., Sieron, A.L., Li, S.W., Schwarze, U., Petty, E., Wertelecki, W., et al., 1999. Human Ehlers-Danlos syndrome type VII C and bovine dermatosparaxis are caused by mutations in the procollagen I N-proteinase gene. Am. J. Hum. Genet. 65, 308–317.

Dagoneau, N., Benoist-Lasselin, C., Huber, C., Faivre, L., Megarbane, A., Alswaid, A., et al., 2004. ADAMTS10 mutations in autosomal recessive Weill-Marchesani syndrome. Am. J. Hum. Genet. 75, 801–806.

Llamazares, M., Cal, S., Quesada, V., Lopez-Otin, C., 2003. Identification and characterization of ADAMTS-20 defines a novel subfamily of metalloproteinases-disintegrins with multiple thrombospondin-1 repeats and a unique GON domain. J. Biol. Chem. 278, 13382–13389.

Rao, C., Foernzler, D., Loftus, S.K., Liu, S., McPherson, J.D., Jungers, K.A., et al., 2003. A defect in a novel ADAMTS family member is the cause of the belted white-spotting mutation. Development 130, 4665–4672.

Shindo, T., Kurihara, H., Kuno, K., Yokoyama, H., Wada, T., Kurihara, Y., et al., 2000. ADAMTS-1: a metalloproteinase-disintegrin essential for normal growth, fertility, and organ morphology and function. J. Clin. Invest. 105, 1345–1352.

Shinomura, T., Nishida, Y., Ito, K., Kimata, K., 1993. cDNA cloning of PG-M, a large chondroitin sulfate proteoglycan expressed during chondrogenesis in chick limb buds. Alternative spliced multiforms of PG-M and their relationships to versican. J. Biol. Chem. 268, 14461–14469.

Somerville, R.P., Longpre, J.M., Jungers, K.A., Engle, J.M., Ross, M., Evanko, S., et al., 2003. Characterization of ADAMTS-9 and ADAMTS-20 as a distinct ADAMTS subfamily related to *Caenorhabditis elegans* GON-1. J. Biol. Chem. 278, 9503–9513.

Somerville, R.P., Jungers, K.A., Apte, S.S., 2004. ADAMTS10: discovery and characterization of a novel, widely expressed metalloprotease and its proteolytic activation. J. Biol. Chem. 279, 51208–51217.

Zheng, X., Chung, D., Takayama, T.K., Majerus, E.M., Sadler, J.E., Fujikawa, K., 2001. Structure of von Willebrand factor cleaving protease (ADAMTS13), a metalloprotease involved in thrombotic thrombocytopenic purpura. J. Biol. Chem. 13, 13.